Hirai et al., 2018, Breakdown of residual zircon in the Izu arc subducting slab during backarc rifting: Geology, https://doi.org/10.1130/G39856.1.

Analytical Procedures

Concentrations of major elements and selected trace elements (Ba, Cr, Ni, Rb, Sr, Zr, Y, and V) in 27 samples were determined on fused glass beads using X-ray fluorescence spectrometry (PANalytical MagiX) at the Hokkaido Education University. Trace element concentrations, including rare earth elements (REEs), were analyzed by inductively coupled plasma mass spectrometry (ICP-MS) on an X-Series 2 (Thermo Fisher Scientific) at the University of the Ryukyus, and on an Agilent 7500a at Niigata University. The analytical uncertainties (1σ) on standards (BHVO-2, JA-1) are shown in Supplementary Table DR1. Isotopic measurements were carried out on a Neptune Plus multi-collector ICP-MS (Thermo Fisher Scientific) at the University of the Ryukyus for Sr, Nd, and Hf, and a Finnigan MAT 262 thermal ionization mass spectrometry (TIMS) at Niigata University for Sr and Nd. The mean values of NIST SRM-987 and JNdi-1 analyzed by multi-collector ICP-MS were found to be $^{87}Sr/^{86}Sr = 0.710256 \pm 0.000016$ (2SD, n = 44) and $^{143}Nd/^{144}Nd = 0.512116 \pm 0.000019$ (2SD, n = 22), respectively. The mean values of NIST SRM-987 and JNdi-1 analyzed by TIMS were found to be $^{87}Sr/^{86}Sr = 0.7102220 \pm 0.000049$ (2SD, n = 14) and $^{143}Nd/^{144}Nd = 0.512088 \pm 0.000018$ (2SD, n = 12), respectively. The Specpurer® Hf Plasma standard solution analyzed by multi-collector ICP-MS during this work was found to be $^{176}Hf/^{177}Hf = 0.282160 \pm 0.000016$ (2SD, n = 13). The uncertainties of individual analysis are represented by 2SE (2 standard error) in Table DR1.

Slab Melt Modeling

Concentrations in slab melts used partition coefficients and mineral modes provided in Table DR2, and shown in Table DR3 with end-member compositions. Modal compositions of mineral phases in the slab were assumed based on experiments on slab-melting at eclogitic conditions (3.5–4.0 GPa; Schmidt et al., 2004). Partition coefficients for slab melting are from experimental data (Johnson, 1998; Foley et al., 2000; Rubatto and Hermann, 2007; Skora and Blundy, 2010). Melting assumes 10% non-modal batch melting (garnet:cpx = 50:50 for melting). We assumed that the slab is composed of altered oceanic crust and sediment in a 9:1 ratio, which is based on previous assumptions for the Izu arc (Tollstrup et al., 2010; Freymuth et al., 2016). Two types of sediments on the subducting Pacific plate, pelagic and volcanogenic, were discovered at ODP site 801 (Karl et al., 1992) and site 1149 (Plank et al., 2007), but it is difficult to determine their relative proportions. Here, we assumed that the sediments contributed to the source of the active rift basalts in a 5:5 pelagic to volcanogenic ratio. Pelagic sediment compositions were based on data in Plank et al. (2007) and Chauvel et al. (2009). Volcanogenic sediment compositions were based on data in Pearce et al. (1999) and Plank and Langmuir (1998). Trace element concentrations of the mantle wedge were from Workman and Hart (2005), and its isotopic compositions were assumed based on the Izu-Bonin-Mariana (IBM) sub-arc mantle array (Freymuth et al., 2016) using data from IBM back-arc basins (Straub et al., 2010; Tollstrup et al., 2010; Woodhead et al., 2012). Altered oceanic crust compositions were based on data in Hauff et al. (2003) and Miyazaki et al. (2015).

REFERENCE CITED

Chauvel, C., Marini, J.C., Plank, T., and Ludden, J.N., 2009, Hf-Nd input flux in the Izu-Mariana subduction zone and recycling of subducted material in the mantle: Geochemistry, Geophysics, Geosystems, v. 10, p. 1–23, doi: 10.1029/2008GC002101.

Foley, S.F., Barth, M.G., and Jenner, G.A., 2000, Rutile/melt partition coefficients for trace elements and an assessment of the influence of rutile on the trace element characteristics of subduction zone magmas: Geochimica et Cosmochimica Acta, v. 64, p. 933–938, doi: 10.1016/S0016-7037(99)00355-5.

Freymuth, H., Ivko, B., Gill, J.B., Tamura, Y., and Elliott, T., 2016, Thorium isotope evidence for melting of the mafic oceanic crust beneath the Izu arc: Geochimica et Cosmochimica Acta, v. 186, p. 49–70, doi: 10.1016/j.gca.2016.04.034.

Fryer, P., Taylor, B., Langmuir, C.H., and Hochstaedter, A.G., 1990, Petrology and geochemistry of lavas from the Sumisu and Torishima backarc rifts: Earth and Planetary Science Letters, v. 100, p. 161–178, doi: 10.1016/0012-821X(90)90183-X.

Gill, J.B., Seales, C., Thompson, P., Hochstaedter, A.G., and Dunlap, C., 1992, Petrology and geochemistry of Pliocene-Pleistocene volcanic rocks from the Izu Arc, Leg 126, in Proceedings of the Ocean Drilling Program, Scientific Results, v. 126, p. 383–404.

Hauff, F., Hoernle, K., and Schmidt, A., 2003, Sr-Nd-Pb composition of Mesozoic Pacific oceanic crust (Site 1149 and 801, ODP Leg 185): Implications for alteration of ocean crust and the input into the Izu-Bonin-Mariana subduction system: Geochemistry, Geophysics, Geosystems, v. 4, doi: 10.1029/2002GC000421.

Hochstaedter, A.G., Gill, J.B., Kusakabe, M., Newman, S., Pringle, M., Taylor, B., and Fryer, P., 1990a, Volcanism in the Sumisu Rift, I. Major element, volatile, and stable isotope

geochemistry: Earth and Planetary Science Letters, v. 100, p. 179–194, doi: 10.1016/0012-821X(90)90184-Y.

Hochstaedter, A.G., Gill, J.B., and Morris, J.D., 1990b, Volcanism in the Sumisu Rift, II. Subduction and non-subduction related components: Earth and Planetary Science Letters, v. 100, p. 195–209, doi: 10.1016/0012-821X(90)90185-Z.

Ikeda, Y., and Yuasa, M., 1989, Volcanism in nascent back-arc basins behind the Shichito Ridge and adjacent areas in the Izu-Ogasawara arc, northwest Pacific: evidence for mixing between E-type MORB and island arc magmas at the initiation of back-arc rifting: Contributions to Mineralogy and Petrology, v. 101, p. 377–393, doi: 10.1007/BF00372212.

Isse, T., Shiobara, H., Tamura, Y., Suetsugu, D., Yoshizawa, K., Sugioka, H., Ito, A., Kanazawa, T., Shinohara, M., Mochizuki, K., Araki, E., Nakahigashi, K., Kawakatsu, H., Shito, A., et al., 2009, Seismic structure of the upper mantle beneath the Philippine Sea from seafloor and land observation: Implications for mantle convection and magma genesis in the Izu-Bonin-Mariana subduction zone: Earth and Planetary Science Letters, v. 278, p. 107–119, doi: 10.1016/j.epsl.2008.11.032.

Johnson, K.T.M., 1998, Experimental determination of partition coefficients for rare earth and high-field-strength elements between clinopyroxene, garnet, and basaltic melt at high pressures: Contributions to Mineralogy and Petrology, v. 133, p. 60–68, doi: 10.1007/s004100050437.

Karl, S.M., Wandless, G. a, and Karpoff, a M., 1992, Sedimentological and geochemical characteristics of Leg 129 siliceous deposits., in In Larson R.L., Lancelot Y. et al., Proceedings ODP, Scientific Results, 129, College Station, TX (Ocean Drilling Program), v. 129, p. 31–79.

Miyazaki, T., Kimura, J.-I., Senda, R., Vaglarov, B.S., Chang, Q., Takahashi, T., Hirahara, Y., Hauff, F., Hayasaka, Y., Sano, S., Shimoda, G., Ishizuka, O., Kawabata, H., Hirano, N., et al., 2015, Missing western half of the Pacific Plate: Geochemical nature of the Izanagi-Pacific Ridge interaction with a stationary boundary between the Indian and Pacific mantles: Geochemistry, Geophysics, Geosystems, v. 16, p. 3309–3332, doi: 10.1002/2015GC005911.

Obana, K., Kamiya, S., Kodaira, S., Suetsugu, D., Takahashi, N., Takahashi, T., and Tamura, Y., 2010, Along-arc variation in seismic velocity structure related to variable growth of arc crust in northern Izu-Bonin intraoceanic arc: Geochemistry, Geophysics, Geosystems, v. 11, p. 1–13, doi: 10.1029/2010GC003146.

Pearce, J.A., Kempton, P.D., Nowell, G.M., and Noble, S.R., 1999, Hf-Nd element and isotope perspective on the nature and provenance of mantle and subduction components in Western Pacific Arc-Basin systems: Journal of Petrology, v. 40, p. 1579–1611, doi: 10.1093/petroj/40.11.1579.

Pearce, J.A., Stern, R.J., Bloomer, S.H., and Fryer, P., 2005, Geochemical mapping of the Mariana arc-basin system: Implications for the nature and distribution of subduction components: Geochemistry, Geophysics, Geosystems, v. 6, doi: 10.1029/2004GC000895.

Plank, T., Kelley, K.A., Murray, R.W., and Stern, L.Q., 2007, Chemical composition of sediments subducting at the Izu-Bonin trench: Geochemistry, Geophysics, Geosystems, v. 8, p. 1–16, doi: 10.1029/2006GC001444.

Plank, T., and Langmuir, C.H., 1998, The chemical composition of subducting sediment and its consequences for the crust and mantle: Chemical Geology, v. 145, p. 325–394, doi: 10.1016/S0009-2541(97)00150-2.

Rubatto, D., and Hermann, J., 2007, Experimental zircon/melt and zircon/garnet trace element partitioning and implications for the geochronology of crustal rocks: Chemical Geology, v. 241, p. 38–61, doi: 10.1016/j.chemgeo.2007.01.027.

Schmidt, M.W., Vielzeuf, D., and Auzanneau, E., 2004, Melting and dissolution of subducting crust at high pressures: The key role of white mica: Earth and Planetary Science Letters, v. 228, p. 65–84, https://doi.org/10.1016/j.epsl.2004.09.020.

Skora, S., and Blundy, J., 2010, High-pressure hydrous phase relations of radiolarian clay and implications for the involvement of subducted sediment in arc magmatism: Journal of Petrology, v. 51, p. 2211–2243, doi: 10.1093/petrology/egq054.

Straub, S.M., Goldstein, S.L., Class, C., Schmidt, A., and Gomez-Tuena, A., 2010, Slab and mantle controls on the Sr-Nd-Pb-Hf isotope evolution of the Post 42 Ma Izu-Bonin volcanic arc: Journal of Petrology, v. 51, p. 993–1026, doi: 10.1093/petrology/egq009.

Taylor, R.N., and Nesbitt, R.W., 1998, Isotopic characteristics of subduction fluids in an intra-oceanic setting, Izu-Bonin Arc, Japan: Earth and Planetary Science Letters, v. 164, p. 79–98, doi: 10.1016/S0012-821X(98)00182-4.

Tollstrup, D.L., Gill, J., Kent, A.J.R., Prinkey, D., Williams, R., Tamura, Y., and Ishizuka, O., 2010, Across-arc geochemical trends in the Izu-Bonin arc: Contributions from the subducting slab, revisited: Geochemistry, Geophysics, Geosystems, v. 11, doi: 10.1029/2000GC000105.

Woodhead, J., Stern, R.J., Pearce, J., Hergt, J., and Vervoort, J., 2012, Hf-Nd isotope variation in Mariana Trough basalts: The importance of “ambient mantle” in the interpretation of subduction zone magmas: Geology, v. 40, p. 539–542, doi: 10.1130/G32963.1.

Workman, R.K., and Hart, S.R., 2005, Major and trace element composition of the depleted MORB mantle (DMM): Earth and Planetary Science Letters, v. 231, p. 53–72, doi: 10.1016/j.epsl.2004.12.005.

SUPPLEMENTARY FIGURES

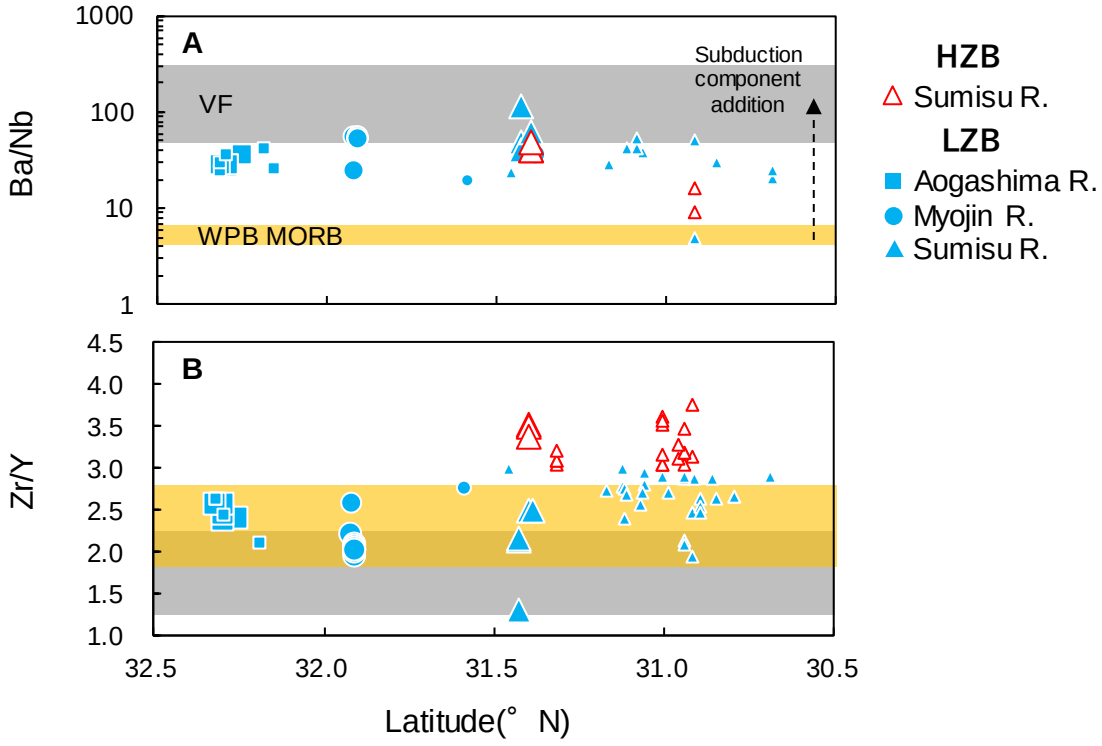

Figure DR1. Along-rift variations in (A) Ba/Nb, and (B) Zr/Y in the active rift basalts. The high Zr/Y basalts (HZB) and low Zr/Y basalts (LZB) are here defined as Zr/Y > 3.0 and Zr/Y ≦3.0, respectively. Large symbols are data from this study, and small symbols are data from previous studies (Ikeda and Yuasa, 1989; Fryer et al., 1990; Hochstaedter et al., 1990a, 1990b, 2001; Gill et al., 1992; Tollstrup et al., 2010). The gray field denotes the range of basalts from the volcanic front (VF; Taylor and Nesbitt, 1998; Tollstrup et al., 2010; Freymuth et al., 2016). Data for the range of mid ocean ridge basalts (MORB)-like basalts from the West Philippine Basin (WPB MORB; orange) are from Pearce et al. (2005). The previous studies contain data analyzed by X-ray fluorescence (XRF) methods.

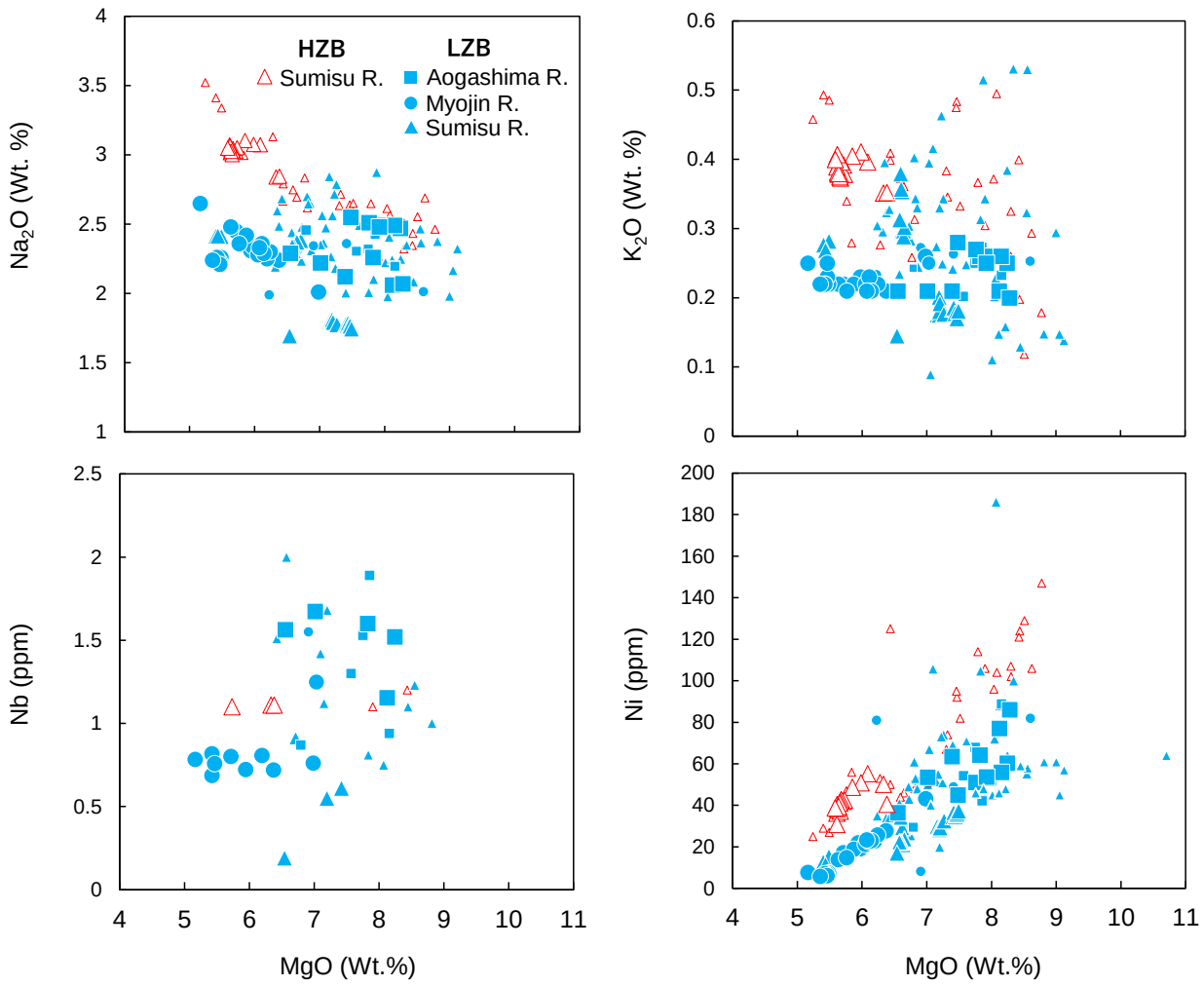

Figure DR2. MgO variation diagram of selected incompatible elements (Na_2O, K_2O, and Nb) and Ni for the active rift basalts. Large symbols are data from this study, and small symbols are data from previous studies (Ikeda and Yuasa, 1989; Fryer et al., 1990; Hochstaedter et al., 1990a, 1990b, 2001; Gill et al., 1992; Tollstrup et al., 2010).

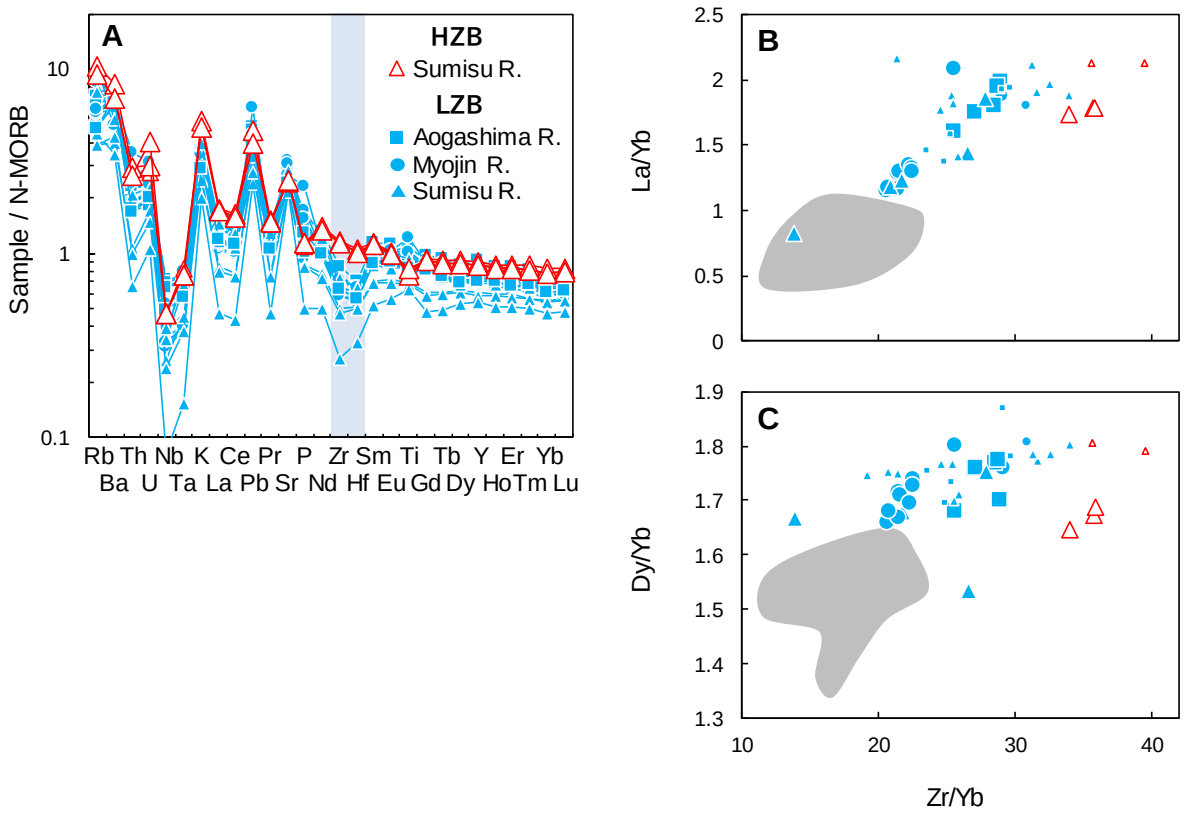

Figure DR3. (A) N-MORB (Sun and McDonough, 1989) normalized trace element diagram (shown only for samples from this study), and (B) La/Yb, and (C) Dy/Yb vs. Zr/Yb plot for the active rift basalts. The Zr/Yb are used as a function for type discrimination. Light blue field in (A) highlights the absence of a negative Zr and Hf concentration anomaly in the HZB (high Zr/Y basalts). Large symbols are data from this study, and small symbols are data from previous studies (Gill et al., 1992; Tollstrup et al., 2010). The gray fields in Figure B and C denote the range of basalts from the volcanic front (Taylor and Nesbitt, 1998; Tollstrup et al., 2010; Freymuth et al., 2016).

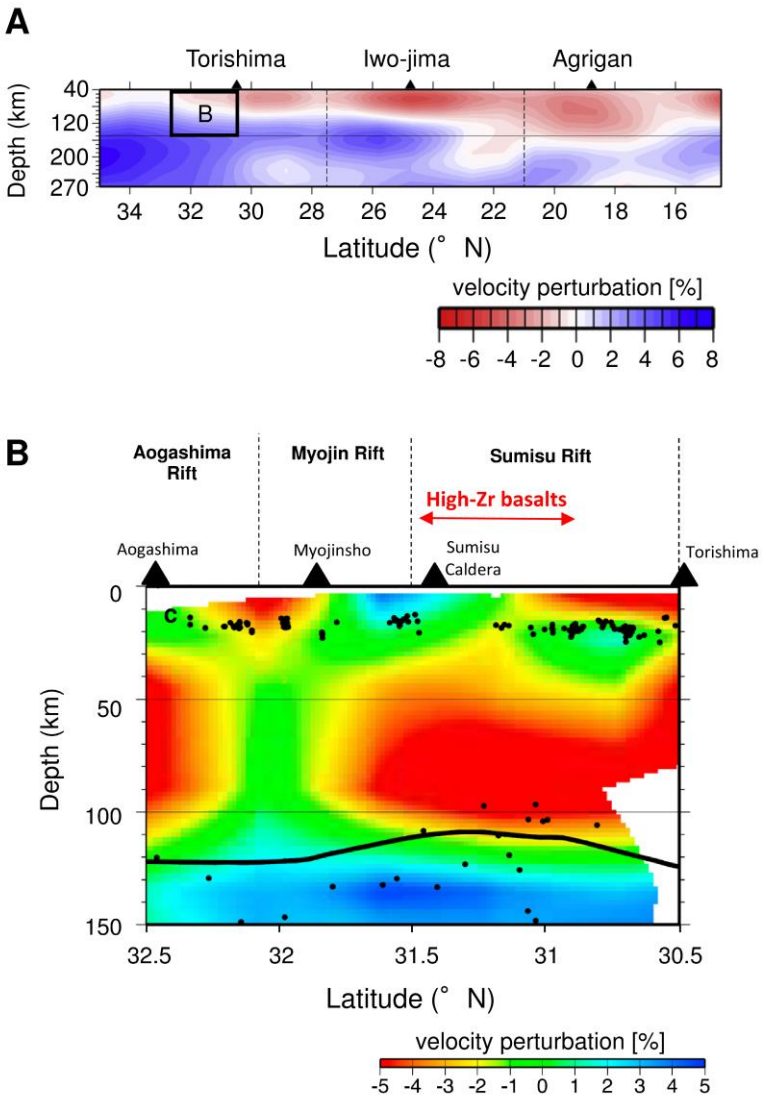

Figure DR4. S-wave velocity perturbations beneath the volcanic front of the Izu-Bonin-Mariana arc. (A) Overview of the Izu-Bonin-Mariana arc after Isse et al. (2009), revealing three slow velocity anomalies in the mantle wedge along the Izu-Bonin-Mariana arc. (B) Area focused on 30.5° to 32.5°N, as shown in the black box in part (A); modified from Obana et al. (2010). Dashed lines represent the inferred boundary of each rift where the S-wave velocity structure is applied to the active rift zone. Black triangles are Quaternary volcanoes. The thick solid line and dots are the top of the subducting Pacific plate and earthquakes within 20 km of the cross section, respectively.

SUPPLEMENTARY TABLES

Table DR1 Chemical, isotopic and modal compositions of volcanic rocks from the active rift zone and volcanic front.

Tectonic settings:	Active rift zone						
Location:	Aogashima Rift					Myojin Rift	
Dredge site:	10TBMD8	10TBMD9	10TBMD9	10TBMD9	10TBMD10	10TBMD3	10TBMD3
Sample:	H05	H06	H12	H20	H03	H01	H20
Latitude (°N):	32.25	32.30	32.30	32.30	32.32	31.92	31.92
Longitude (°E):	139.73	139.72	139.72	139.72	139.73	139.61	139.61
Depth (mbsl):	1595	1353	1353	1353	1353	917	917
Basalt type:	Low-Zr	Low-Zr	Low-Zr	Low-Zr	Low-Zr	Low-Zr	Low-Zr
Major element wt.%							
SiO_2	48.03	48.03	47.77	48.00	48.07	47.68	48.31
TiO_2	1.04	1.08	1.06	0.99	1.05	1.00	1.00
Al_2O_3	16.44	16.85	16.58	17.01	17.70	16.83	17.55
Fe_2O_3	12.20	11.56	11.75	10.71	10.96	11.41	10.09
MnO	0.21	0.28	0.46	0.18	0.18	0.20	0.17
MgO	7.98	6.37	6.82	7.63	8.20	6.85	6.91
CaO	11.27	11.57	11.42	11.59	11.56	13.00	12.69
Na_2O	2.03	2.22	2.15	2.21	2.46	1.97	2.17
K_2O	0.20	0.20	0.21	0.25	0.25	0.25	0.25
P_2O_5	0.15	0.19	0.19	0.16	0.17	0.11	0.12
Total	99.55	98.35	98.42	98.73	100.60	99.30	99.26
Trace element (XRF) ppm							
V	342.9	324.0	320.3	283.1	283.7	338.0	295.4
Cr	214.7	144.9	159.7	200.3	192.7	112.9	145.9
Co	48.3	54.8	56.1	49.0	51.4	48.7	43.8
Ni	77.1	36.5	53.6	64.3	60.4	43.2	52.5
Rb	2.5	2.5	2.9	2.8	2.8	5.0	4.3
Sr	211.9	224.6	222.4	240.0	231.2	275.5	261.6
Ba	42.7	54.2	51.8	55.5	56.7	56.5	44.1
Y	18.8	18.5	19.3	18.1	20.7	16.9	19.2
Zr	48.5	58.6	57.6	55.2	54.8	43.1	55.1
Nb	2.1	3.5	4.1	4.5	0.7	1.8	2.3
Trace element (ICP-MS) ppm							
Li	4.47	5.05	5.81	4.54	3.70	3.94	4.91
Sc	40.2	49.1	50.9	42.4	36.3	47.4	42.1
V	343	368	394	309	274	369	300
Cr							
Co	41.0	36.6	44.5	48.4	39.9	39.8	35.9
Ni							
Rb	2.7	2.7	3.7	4.0	3.6	5.2	4.8
Sr	214.7	229.5	264.5	233.3	231.1	287.5	278.1
Y	19.74	23.88	25.69	20.36	20.11	19.73	20.53
Zr	47.39	56.96	62.90	52.38	52.03	43.64	53.51
Nb	1.15	1.56	1.67	1.60	1.52	0.76	1.25
Cs	0.42	0.22	0.57	0.31	0.27	0.65	1.11
Ba	41.69	44.34	45.84	46.53	44.77	42.77	31.33
La	2.99	3.72	4.01	3.63	3.56	3.58	3.44
Ce	8.42	10.31	11.08	9.36	9.58	9.16	9.06
Pr	1.40	1.74	1.88	1.59	1.60	1.55	1.50
Nd	7.33	8.81	9.62	7.73	8.12	8.41	7.98
Sm	2.32	2.82	3.01	2.46	2.46	2.45	2.41
Eu	0.92	1.04	1.14	0.92	0.95	0.90	0.91
Gd	2.96	3.37	3.56	2.96	3.05	2.99	2.95
Tb	0.50	0.57	0.63	0.49	0.52	0.49	0.51
Dy	3.12	3.70	3.91	3.09	3.23	3.07	3.24
Ho	0.72	0.80	0.86	0.70	0.70	0.68	0.71
Er	1.97	2.30	2.50	1.96	2.01	1.90	2.10
Tm	0.31	0.34	0.37	0.30	0.30	0.29	0.31
Yb	1.85	2.11	2.21	1.81	1.82	1.71	1.84
Lu	0.28	0.32	0.34	0.28	0.28	0.26	0.28
Hf	1.16	1.32	1.44	1.33	1.31	1.11	1.33
Ta	0.08	0.09	0.10	0.10	0.10	0.05	0.08
Pb	1.21	1.46	1.41	1.06	0.76	1.85	1.33
Th	0.20	0.21	0.23	0.29	0.28	0.43	0.29
U	0.09	0.09	0.10	0.11	0.11	0.15	0.11
Isotope							
$^{87}Sr/^{86}Sr$	0.703207	0.703333	0.703325	0.703195	0.703123	0.703199	0.703040
2SE	0.000009	0.000012	0.000012	0.000012	0.000014	0.000012	0.000012
Method	MC-ICP-MS	TIMS	TIMS	TIMS	MC-ICP-MS	TIMS	TIMS
$^{143}Nd/^{144}Nd$	0.513064	0.513065	0.513067	0.513074	0.513075	0.513039	0.513091
2SE	0.000009	0.000014	0.000014	0.000014	0.000010	0.000014	0.000014
Method	MC-ICP-MS	TIMS	TIMS	TIMS	MC-ICP-MS	TIMS	TIMS
$^{176}Hf/^{177}Hf$	0.283211				0.283203		
2SE	0.000009				0.000009		
Method	MC-ICP-MS				MC-ICP-MS		

Table DR1 Chemical, isotopic and modal compositions of volcanic rocks from the active rift zone and volcanic front.

Tectonic settings:	Active rift zone							
Location:	Myojin Rift							
Dredge site:	11TBMD4	11TBMD4	11TBMD4	11TBMD4	11TBMD4	11TBMD4	11TBMD4	11TBMD4
Sample:	H01	H03	H05	H08	H16	H09	H10	H17
Latitude (°N):	31.91	31.91	31.91	31.91	31.91	31.91	31.91	31.91
Longitude (°E):	139.77	139.77	139.77	139.77	139.77	139.77	139.77	139.77
Depth (mbsl):	1209	1209	1209	1209	1209	1209	1209	1209
Basalt type:	Low-Zr	Low-Zr	Low-Zr	Low-Zr	Low-Zr	Low-Zr	Low-Zr	Low-Zr
Major element wt.%								
SiO_2	48.61	48.22	48.94	48.56	49.12	48.35	48.62	48.27
TiO_2	1.29	1.24	1.34	1.25	1.49	1.37	1.39	1.36
Al_2O_3	16.15	16.15	15.87	16.19	15.56	15.48	15.51	15.49
Fe_2O_3	13.56	13.33	13.78	13.44	14.29	15.21	15.21	15.13
MnO	0.23	0.22	0.23	0.23	0.25	0.24	0.26	0.25
MgO	5.82	6.22	5.59	6.08	5.03	5.29	5.31	5.32
CaO	10.95	11.12	10.70	11.18	9.98	10.71	10.71	10.68
Na_2O	2.26	2.19	2.39	2.21	2.58	2.18	2.21	2.15
K_2O	0.21	0.20	0.21	0.21	0.25	0.22	0.22	0.25
P_2O_5	0.18	0.17	0.19	0.18	0.26	0.11	0.11	0.10
Total	99.26	99.07	99.25	99.52	98.81	99.16	99.53	99.01
Trace element (XRF) ppm								
V	408.5	395.1	417.8	410.0	429.7	524.9	528.8	520.6
Cr	35.7	62.0	29.9	49.4	12.8	18.7	17.6	19.4
Co	59.4	59.4	60.9	60.4	61.2	65.5	65.6	66.3
Ni	22.0	27.8	17.2	22.8	7.7	7.1	7.2	6.2
Rb	4.1	2.3	3.4	3.5	4.6	3.0	2.6	5.2
Sr	224.2	220.2	222.2	221.1	230.3	204.1	204.9	206.5
Ba	44.7	40.0	43.9	42.0	40.3	42.7	47.0	45.8
Y	20.2	22.0	22.8	20.2	24.9	21.6	21.4	17.3
Zr	47.1	44.9	49.7	46.7	53.7	45.2	44.8	43.9
Nb	-	-	-	-	1.2	-	-	1.5
Trace element (ICP-MS) ppm								
Li	3.86	3.89	4.25	4.37	4.48	4.03	3.64	3.56
Sc	37.6	44.7	42.3	45.7	47.5	48.1	59.2	49.0
V	366	414	409	415	439	484	582	505
Cr								
Co	38.2	37.7	36.3	76.0	39.4	35.4	41.0	35.3
Ni								
Rb	2.9	3.2	3.2	3.3	3.4	2.7	3.1	3.5
Sr	208.7	229.6	223.7	234.4	238.4	188.2	213.1	189.2
Y	20.96	21.66	22.79	22.51	23.32	19.96	22.88	20.44
Zr	42.41	43.69	47.95	46.59	48.05	39.04	45.55	41.38
Nb	0.72	0.72	0.80	0.81	0.78	0.69	0.82	0.76
Cs	0.13	0.15	0.15	0.30	0.13	0.16	0.20	0.18
Ba	38.96	39.44	43.28	45.62	41.91	38.71	43.19	40.33
La	2.57	2.66	2.93	2.77	2.81	2.21	2.51	2.36
Ce	7.47	7.57	8.06	7.89	8.05	6.38	7.25	6.64
Pr	1.34	1.36	1.43	1.39	1.44	1.11	1.25	1.15
Nd	6.95	7.33	7.68	7.46	7.70	5.80	6.68	6.31
Sm	2.30	2.40	2.58	2.50	2.53	2.01	2.37	2.20
Eu	0.98	1.00	1.05	1.05	1.06	0.84	0.97	0.86
Gd	3.12	3.03	3.38	3.21	3.25	2.63	3.07	2.88
Tb	0.52	0.53	0.59	0.57	0.57	0.49	0.54	0.51
Dy	3.41	3.48	3.67	3.61	3.70	3.16	3.56	3.36
Ho	0.77	0.78	0.83	0.78	0.83	0.73	0.80	0.73
Er	2.18	2.16	2.39	2.27	2.31	2.01	2.28	2.15
Tm	0.32	0.33	0.35	0.35	0.36	0.32	0.35	0.33
Yb	1.99	2.04	2.16	2.07	2.14	1.90	2.13	2.00
Lu	0.29	0.30	0.31	0.31	0.31	0.28	0.32	0.29
Hf	1.19	1.14	1.27	1.20	1.26	1.05	1.21	1.13
Ta	0.05	0.05	0.06	0.11	0.05	0.05	0.05	0.05
Pb	1.11	0.94	1.14	1.04	1.07	0.88	1.14	1.01
Th	0.21	0.20	0.23	0.22	0.23	0.18	0.20	0.18
U	0.10	0.09	0.10	0.10	0.10	0.08	0.09	0.09
Isotope								
$^{87}Sr/^{86}Sr$		0.703246	0.703233		0.703306	0.703390	0.703382	0.703368
2SE		0.000014	0.000013		0.000010	0.000014	0.000011	0.000014
Method		TIMS	TIMS		TIMS	TIMS	TIMS	TIMS
$^{143}Nd/^{144}Nd$		0.513078	0.513065		0.513077	0.513081	0.513065	0.513072
2SE		0.000014	0.000014		0.000014	0.000014	0.000014	0.000014
Method		TIMS	TIMS		TIMS	TIMS	TIMS	TIMS
$^{176}Hf/^{177}Hf$		0.283206	0.283214			0.283207		
2SE		0.000009	0.000011			0.000014		
Method		MC-ICP-MS	MC-ICP-MS			MC-ICP-MS		

Table DR1 Chemical, isotopic and modal compositions of volcanic rocks from the active rift zone and volcanic front.

Tectonic settings:	Active rift zone							
Location:	Sumisu Rift							
Dredge site:	14TBMD7	14TBMD7	14TBMD7	14TBMD8	14TBMD8	14TBMD8	16TBMD1	16TBMD3
Sample:	H07	H08	H1R	H04	H13	H12R	H04	H06
Latitude (°N):	31.40	31.40	31.40	31.43	31.43	31.43	31.40	31.39
Longitude (°E):	139.78	139.78	139.78	139.84	139.84	139.84	139.69	139.73
Depth (mbsl):	1480	1480	1480	1337	1337	1337	1404	1505
Basalt type:	High-Zr	High-Zr	High-Zr	Low-Zr	Low-Zr	Low-Zr	Low-Zr	Low-Zr
Major element wt.%								
SiO_2	52.68	54.29	51.50	48.54	49.02	48.26	50.24	48.44
TiO_2	1.03	0.95	1.01	0.80	0.88	0.84	1.06	1.17
Al_2O_3	16.90	16.82	16.27	18.07	17.23	16.95	16.27	16.14
Fe_2O_3	10.05	9.64	10.07	12.66	11.13	11.17	12.58	12.83
MnO	0.18	0.18	0.18	0.21	0.19	0.20	0.28	0.23
MgO	6.35	5.73	6.19	6.55	7.43	7.00	5.36	6.59
CaO	10.26	9.38	10.10	12.27	12.79	12.39	10.43	11.37
Na_2O	2.89	3.09	2.76	1.72	1.81	1.74	2.36	2.34
K_2O	0.35	0.38	0.34	0.15	0.18	0.18	0.28	0.28
P_2O_5	0.13	0.13	0.13	0.06	0.10	0.09	0.12	0.15
Total	100.80	100.59	98.55	101.03	100.76	98.82	98.98	99.55
Trace element (XRF) ppm								
V	268.5	235.5	272.4	360.6	330.9	319.6	380.7	354.1
Cr	132.7	106.4	138.3	24.6	89.6	59.3	57.2	39.4
Co	41.4	39.6	42.0	52.5	46.0	46.9	52.2	53.2
Ni	52.5	44.7	41.2	17.7	37.3	30.7	15.3	26.8
Rb	5.3	7.0	6.0	2.6	1.7	2.3	5.0	6.8
Sr	228.6	223.3	228.1	197.2	201.2	201.9	218.4	255.3
Ba	36.4	71.7	77.4	31.0	12.1	47.6	63.6	55.1
Y	19.8	24.2	25.4	10.8	15.8	13.3	22.9	22.1
Zr	81.0	85.7	83.9	27.4	42.1	40.8	54.2	55.2
Nb	3.6	1.9	0.0	-	2.8	0.2	1.7	2.4
Trace element (ICP-MS) ppm								
Li	5.50	5.90	5.00	5.30	3.20	3.60		
Sc	38.8	35.9	40.2	51.3	53.9	50.3	36.5	31.3
V	280	258	286	378	335	332	407	374
Cr	107	78	118	17	78	42	42.3	41.7
Co	36.0	32.0	36.0	46.0	44.0	43.0	39.1	45.6
Ni	51	42	51	20	38	32		
Rb	5.4	5.9	5.3	2.5	2.2	2.2	4.3	5.7
Sr	228.0	220.0	226.0	197.0	201.0	198.0	215.8	253.9
Y	24.10	25.40	24.30	15.20	17.10	16.40	21.38	21.63
Zr	85.00	86.00	85.00	20.00	37.00	35.00	53.77	54.16
Nb	1.11	1.10	1.11	0.19	0.61	0.55	0.80	0.91
Cs	0.37	0.28	0.29	0.28	0.17	0.17	0.20	0.23
Ba	44.00	53.00	44.00	22.00	25.00	27.00	48.57	33.63
La	4.25	4.40	4.24	1.19	2.10	1.98	2.93	3.61
Ce	11.94	12.33	11.95	3.25	5.90	5.63	8.05	9.60
Pr	1.94	1.99	1.95	0.62	1.03	0.98	1.42	1.71
Nd	9.88	10.15	9.84	3.67	5.66	5.33	7.21	8.79
Sm	2.94	3.03	2.93	1.36	1.87	1.83	2.27	2.67
Eu	1.00	1.03	1.01	0.58	0.73	0.70	0.84	1.02
Gd	3.36	3.46	3.37	1.76	2.27	2.18	3.03	3.23
Tb	0.59	0.62	0.59	0.33	0.41	0.40	0.51	0.56
Dy	3.98	4.16	4.00	2.40	2.85	2.79	3.10	3.41
Ho	0.85	0.88	0.84	0.52	0.61	0.60	0.69	0.77
Er	2.47	2.57	2.48	1.52	1.77	1.73	2.18	2.22
Tm	0.37	0.39	0.37	0.23	0.26	0.26	0.29	0.32
Yb	2.38	2.53	2.37	1.44	1.70	1.67	2.03	1.94
Lu	0.36	0.38	0.36	0.22	0.25	0.25	0.32	0.32
Hf	2.10	2.16	2.09	0.68	1.04	1.03	1.33	1.33
Ta	0.11	0.10	0.10	0.02	0.06	0.05	0.09	0.09
Pb	1.37	1.41	1.20	0.72	0.83	0.89	1.02	0.83
Th	0.32	0.35	0.32	0.08	0.13	0.12	0.25	0.31
U	0.13	0.14	0.19	0.05	0.08	0.07	0.11	0.14
Isotope								
$^{87}Sr/^{86}Sr$	0.703009	0.703036	0.702989	0.703316	0.703148	0.703198	0.703257	0.703006
2SE	0.000010	0.000009	0.000009	0.000008	0.000011	0.000010	0.000014	0.000020
Method	MC-ICP-MS	MC-ICP-MS	MC-ICP-MS	MC-ICP-MS	MC-ICP-MS	MC-ICP-MS	TIMS	TIMS
$^{143}Nd/^{144}Nd$	0.513102	0.513097	0.513099	0.513104	0.513098	0.513091	0.513056	
2SE	0.000007	0.000007	0.000008	0.000009	0.000008	0.000008	0.000014	
Method	MC-ICP-MS	MC-ICP-MS	MC-ICP-MS	MC-ICP-MS	MC-ICP-MS	MC-ICP-MS	TIMS	
$^{176}Hf/^{177}Hf$	0.283213	0.283213	0.283201	0.283251	0.283222	0.283217		
2SE	0.000013	0.000013	0.000017	0.000009	0.000008	0.000009		
Method	MC-ICP-MS	MC-ICP-MS	MC-ICP-MS	MC-ICP-MS	MC-ICP-MS	MC-ICP-MS		

Table DR1 Chemical, isotopic and modal compositions of volcanic rocks from the active rift zone and volcanic front.

Tectonic settings:	Volcanic front			
Location:	Myojinsho			
Dredge site:	1970D4	1970D4	1970D4	13TBMD2
Sample:	H02	H03	H04	H01
Latitude (°N):	31.98	31.98	31.98	31.89
Longitude (°E):	139.85	139.85	139.85	139.95
Depth (mbsl):	1170	1170	1170	453
Basalt type:	VF	VF	VF	VF
Major element wt.%				
SiO_2	49.43	49.43	49.44	47.29
TiO_2	1.24	1.25	1.25	0.82
Al_2O_3	15.17	15.24	15.20	16.25
Fe_2O_3	15.28	15.22	15.16	13.93
MnO	0.24	0.24	0.24	0.19
MgO	5.25	5.00	5.13	6.68
CaO	10.39	10.31	10.37	12.47
Na_2O	2.21	2.24	2.22	1.33
K_2O	0.21	0.22	0.20	0.26
P_2O_5	0.08	0.09	0.08	0.05
Total	99.50	99.23	99.31	99.29
Trace element (XRF) ppm				
V	486.1	486.6	482.3	545.1
Cr	24.8	17.3	17.6	34.1
Co	60.4	58.8	58.5	54.3
Ni	10.6	5.1	7.4	19.1
Rb	3.8	3.2	3.4	4
Sr	178.4	179.9	180.3	159.3
Ba	53.5	57.5	54	53.8
Y	20.1	20.9	21	14.6
Zr	36.6	36.7	37.7	26.0
Nb	0.2	-	0.5	-
Trace element (ICP-MS) ppm				
Li	5.80	3.98	5.03	3.24
Sc	57.3	56.5	50.7	59.7
V	564	513	523	592
Cr				
Co	43.9	40.2	40.0	45.8
Ni				
Rb	2.7	2.6	2.6	3.8
Sr	188.5	171.5	183.2	161.4
Y	21.89	20.83	21.09	14.13
Zr	36.68	35.00	33.72	20.33
Nb	0.45	0.41	0.43	0.17
Cs	0.21	0.19	0.20	0.82
Ba	50.20	47.03	49.27	45.12
La	1.84	1.75	1.71	1.23
Ce	5.32	5.03	5.17	3.31
Pr	0.98	0.95	0.98	0.59
Nd	5.35	5.28	5.48	3.46
Sm	2.00	1.93	1.98	1.31
Eu	0.84	0.79	0.85	0.51
Gd	2.70	2.65	2.74	1.75
Tb	0.49	0.48	0.50	0.32
Dy	3.28	3.17	3.19	2.12
Ho	0.74	0.71	0.73	0.49
Er	2.17	2.15	2.10	1.41
Tm	0.32	0.32	0.33	0.22
Yb	2.03	1.97	2.00	1.33
Lu	0.31	0.31	0.31	0.21
Hf	1.07	1.00	1.09	0.66
Ta	0.03	0.03	0.03	0.01
Pb	1.61	1.36	1.44	0.78
Th	0.14	0.13	0.13	0.13
U	0.08	0.08	0.08	0.06
Isotope				
$^{87}Sr/^{86}Sr$	0.703540	0.703677	0.703535	0.703603
2SE	0.000013	0.000012	0.000008	0.000011
Method	TIMS	TIMS	MC-ICP-MS	MC-ICP-MS
$^{143}Nd/^{144}Nd$	0.513104	0.513081	0.513083	0.513090
2SE	0.000014	0.000014	0.000014	0.000012
Method	TIMS	TIMS	MC-ICP-MS	MC-ICP-MS
$^{176}Hf/^{177}Hf$			0.283215	0.283221
2SE			0.000009	0.000009
Method			MC-ICP-MS	MC-ICP-MS

Table DR1 Chemical, isotopic and modal compositions of volcanic rocks from the active rift zone and volcanic front.

Tectonic settings:	Standards					
Location:						
Dredge site:						
Sample:	BHVO-2				JA-1	
Latitude (°N):						
Longitude (°E):						
Depth (mbsl):						
Basalt type:						
Major element wt.%						
SiO_2						
TiO_2						
Al_2O_3						
Fe_2O_3						
MnO						
MgO						
CaO						
Na_2O						
K_2O						
P_2O_5						
Total						
Trace element (XRF) ppm						
V						
Cr						
Co						
Ni						
Rb						
Sr						
Ba						
Y						
Zr						
Nb	Niigata Univ.		Univ. Ryukyus		Univ. Ryukyus	
Trace element (ICP-M	(n=4)	(1σ)	(n=4)	(1σ)	(n=4)	(1σ)
Li	4.73	0.16	4.50	0.00	11.20	0.07
Sc	30.9	1.0	31.5	0.9	30.4	0.6
V	312	10	315	2	111	0
Cr			285.8	2.3	6.0	0.0
Co	44	1.4	45	0.4	11	0.0
Ni			113.5	1.1	2.0	0.0
Rb	9.31	0.30	9.2	0.08	11.2	0.07
Sr	382	12	384	2	259	1
Y	27	0.9	27.1	0.3	30.7	0.2
Zr	176.5	5.6	173.5	1.1	83.3	1.6
Nb	19.12	0.60	18.13	0.12	1.30	0.01
Cs	0.098	0.003	0.093	0.004	0.628	0.004
Ba	130.7	4.2	124.8	1.1	252.2	1.9
La	15.2	0.48	15.1	0.06	5.0	0.02
Ce	37.3	1.18	37.0	0.21	11.1	0.07
Pr	5.4	0.17	5.3	0.03	2.1	0.01
Nd	24.26	0.77	24.61	0.16	11.15	0.06
Sm	6.07	0.19	6.12	0.04	3.48	0.03
Eu	2.02	0.07	2.01	0.02	1.13	0.01
Gd	6.10	0.20	6.25	0.03	4.06	0.03
Tb	0.934	0.029	0.935	0.005	0.720	0.007
Dy	5.16	0.16	5.37	0.02	4.93	0.04
Ho	0.982	0.030	0.983	0.008	1.043	0.008
Er	2.51	0.08	2.53	0.02	3.07	0.02
Tm	0.344	0.011	0.348	0.004	0.468	0.004
Yb	1.94	0.06	2.06	0.02	3.00	0.02
Lu	0.273	0.009	0.283	0.004	0.450	0.007
Hf	4.23	0.13	4.42	0.05	2.52	0.03
Ta	1.18	0.04	1.34	0.01	0.12	0.00
Pb	1.47	0.04	3.11	0.03	5.78	0.05
Th	1.238	0.037	1.208	0.011	0.748	0.008
U	0.413	0.012	0.415	0.005	0.355	0.005
Isotope			(n=1)		(n=1)	
$^{87}Sr/^{86}Sr$			0.703473		0.703545	
2SE			0.000009		0.000008	
Method			MC-ICP-MS		MC-ICP-MS	
$^{143}Nd/^{144}Nd$			0.512990		0.513094	
2SE			0.000008		0.000007	
Method			MC-ICP-MS		MC-ICP-MS	
$^{176}Hf/^{177}Hf$			0.283087		0.283259	
2SE			0.000008		0.000007	
Method			MC-ICP-MS		MC-ICP-MS	

Table DR2. Mineral mode of slab and mineral-melt partition coefficients used to calculate bulk distribution coefficients in modeling slab melting.

	cpx	garnet	rutile	zircon	monazite
Mode (vol. %)	60	39	1	0.0 - 0.05	0.0001
Zr	0.119	0.27	3.79	2005	0[a]
Nb	0.004	0.0031	540	0[a]	0[a]
Nd	0.178	0.052	0.684	8.5	1670
Sm	0.293	0.25	2.4	16	1220
Yb	0.4	6.6	0.0158	345	0[a]
Hf	0.2	0.24	4.61	3476	0[a]
Reference	Johnson (1998)	Johnson (1998)	Foley et al. (2000)	Rubatto and Hermann (2007)	Skora and Blundy (2010)

[a]In cases where mineral-melt parition coefficients for some elements were not reported, these are set to zero.

Table DR3. End-member compositions used in mixing models.

		Subducting materials					Calculated slab melts		
	Mantle wedge	Altered oceanic crust	Pelagic sediment	Volcanogenic sediment	Mixed sediment[a]	Slab[b]	Residual zircon 0.05 %	Residual zircon 0.01 %	Residual zircon 0 %
Zr (ppm)	4.27	165.79	55.30	144.20	99.75	159.18	122.67	321.16	539.33
Nb (ppm)	0.09	5.83	5.22	23.75	14.49	6.69	1.22	1.22	1.22
Nd (ppm)	0.48	15.77	25.20	20.17	22.69	16.46	72.08	73.17	73.44
Sm (ppm)	0.21	5.30	5.32	4.07	4.70	5.24	13.82	14.06	14.12
Yb (ppm)	0.35	4.79	2.53	1.20	1.87	4.50	1.64	1.73	1.75
Hf (ppm)	0.13	4.31	1.44	3.79	2.62	4.14	1.99	6.04	12.25
$^{143}Nd/^{144}Nd$	0.51316	0.513147	0.512336	0.512815	0.512549	0.513065	0.513065	0.513065	0.513065
$^{176}Hf/^{177}Hf$	0.28326	0.283182	0.282897	0.282821	0.282842	0.283160	0.283160	0.283160	0.283160
Nb/Yb	0.25	1.22	2.06	19.79	7.77	1.49	0.74	0.70	0.69
Zr/Yb	12.27	34.60	21.86	120.17	53.49	35.38	74.62	185.50	307.38
Nd/Hf	3.80	3.66	17.50	5.32	8.67	3.98	36.17	12.12	6.00
Hf/Hf*	1.00	1.19	0.31	1.03	0.62	1.12	0.15	0.46	0.93

[a]Mixed 50 % pelagic sediment with 50 % volcanogenic sediment.

[b]Composed of 90 % altered oceanic crust and 10 % mixed sediment.